Like-charge attraction in a slit system: pressure components for the primitive model and molecular solvent simulations

2008 J. Phys.: Condens. Matter 20 494235

(http://iopscience.iop.org/0953-8984/20/49/494235)

IOP Publishing Journal of Physics: Condensed Matter

J. Phys.: Condens. Matter **20** (2008) 494235 (12pp) doi:10.1088/0953-8984/20/49/494235

Like-charge attraction in a slit system: pressure components for the primitive model and molecular solvent simulations

Luís Pegado[1], Bo Jönsson[2] and Håkan Wennerström[1]

[1] Physical Chemistry 1, Center for Chemistry and Chemical Engineering, Lund University, POB 124, SE-22100, Sweden

[2] Theoretical Chemistry, Center for Chemistry and Chemical Engineering, Lund University, POB 124, SE-22100, Sweden

E-mail: Luis.Pegado@fkem1.lu.se

Received 21 July 2008, in final form 2 October 2008
Published 12 November 2008
Online at stacks.iop.org/JPhysCM/20/494235

Abstract

We have recently reported Monte Carlo simulations for a system of two infinite like-charged plates in a dipolar fluid solvent (Pegado *et al* 2008 *J. Chem. Phys.* at press). The pressure as a function of plate separation qualitatively reproduces the ion–ion correlation attraction picture seen in primitive model studies, where the solvent only enters the picture implicitly through its dielectric constant ϵ_r, scaling all charge–charge interactions. Here we analyse in detail the different components of the pressure between the two plates. This shows that, by changing any of the relevant parameters (counterion valency, surface charge density or dielectric screening), the appearance or increase of a pressure minimum is connected to the same components in both the primitive model and the dipolar solvent model. Decomposing the pressure is helpful in distinguishing between solvent depletion or packing effects and the coexisting correlation attraction. Although the pressure can be evaluated at any plane parallel to the surfaces, the analysis of the pressure at the midplane provides the best physical insight.

(Some figures in this article are in colour only in the electronic version)

1. Introduction

Ion–ion correlation attraction has been known at least since the early 1980s, when a great deal of theoretical work was done in the context of the primitive model (PM) of electrolyte solutions (e.g. [1, 2]). It is nowadays a well-established phenomenon and an important extension of the DLVO [3] theory of colloid stability. An introduction to the subject can be found in [4], where both theoretical work and experimental manifestations are covered. The systematic theoretical analysis of such a phenomenon in a molecular solvent still has a long way to go, however. The statement applies also to the interaction between net charged objects in general. Studies of net charged objects in molecular solvents have had a tendency to concentrate on structural properties, with less emphasis on the force problem. The forces between net charged objects in solution are the governing properties of a particular system, dictating conditions of stability with profound implications, e.g. in colloid science [5]. Structure in such systems is, in fact, nothing but a property derived from the relevant forces. The fundamental importance of this problem of course goes hand in hand with its difficulty. Some attempts have been made [6–12], but the global picture which emerges is far from being clear. Besides the fact that the results are relatively scattered throughout the literature, they tend to be highly model-dependent. It is a safe statement to say that the thorough study of such problems still needs considerable attention.

In a previous publication [13] we have compared the net osmotic pressure between two infinite like-charged plates with neutralizing counterions only in the primitive model and in a molecular medium sharing a common PM description. The solvent was described using the Stockmayer fluid model, based on an ideal dipole plus a Lennard-Jones potential. This description was kept intentionally simple. The purpose was to depart from the primitive model in a controlled fashion, and to include molecular detail in the solvent in such a way that it was possible to assess whether or not ion–ion correlation attraction is present. A second pressing question was to assess how well

the dielectric screening from a dipolar fluid, strictly dependent on the strength of its dipole moment μ and on its bulk chemical potential, conformed to the bulk dielectric screening constant ϵ_r used in the PM throughout the whole range of plate–plate separations.

The results showed that the molecularity of the solvent as expected enters the picture, and the pressure curves are markedly non-monotonic. This masks, but does not erase, the correlation attraction, which is still present. The manifestation is as usual in the form of a short range attractive pressure minimum, occurring for sufficiently high counterion valency, surface charge density and low enough dielectric screening. This minimum is lost or reduced upon decreasing the electrostatic coupling through any of these three parameters. The analysis of interaction free energies, rather than pressures, unequivocally established the similarity between the models.

In order to further substantiate our point, some general conclusions were given regarding the analysis of pressure components in the PM and in the corresponding Stockmayer fluid description. The relevant data was neither presented nor explored in detail, and the purpose was merely to state that the same components responsible for the correlation attraction in the PM kept their role in the molecular solvent. We nevertheless believe that there is a great deal more to learn about this system by carefully analysing the different pressure components. The possibilities of such a procedure include the separation between correlation and other effects and the connection between the interactions in the system and the different pressure components. Similar net effects are also seen to have a quite distinct physical origin, which also emerges as a result of the analysis. This is so for the case of changing the dielectric screening. In the PM the resulting effect comes about through the direct scaling of all charge–charge interactions by ϵ_r. For a molecular solvent, the separations at which the correlation phenomenon takes place are clearly very far away from those under which the concept of a dielectric constant is derived and applicable, and an extra mechanism is needed to justify a common behaviour with the PM.

A fair share of studies which include pressure decomposition analyses of the ion–ion correlation attraction, in the PM, has previously been done (e.g. [14–19]). These have had the merit of emphasizing that the effect always depends on a balance between entropic and energetic contributions, which is often overlooked. In fact, when doubling the counterion valency at high surface charge density σ and low ϵ_r, the terms which depend on the number of counterions in the system (ideal entropy at the midplane and collision repulsion) change much more drastically (at short range) than the electrostatic attraction [8, 17]. Even if the data is scattered through different sources, and no single systematic study has been done of the behaviour of different components of the pressure upon changing all the relevant parameters (counterion valency q, σ and ϵ_r), the general picture should be well known by now. It obviously lacks, however, a thorough comparative study between the PM and molecular solvent pictures.

One should finally mention Otto and Patey's work on the interaction between like-charge plates [8, 9]. These authors have worked in the context of the anisotropic hypernetted-chain approximation and introduced solvent effects through solvent averaged ion–ion potentials of mean force (PMF). They make a detailed analysis of pressure components, and the final result is that the differences between the PM and their implicit molecular solvent are dominated by an effective pressure term. This is defined as the difference between the total PMF and the screened Coulomb part present in the PM. The results are also shown to be highly model-dependent [9].

2. Model and simulation details

An extensive description of the model, simulations and data evaluation is given in [13]. In particular, we have presented a quite detailed discussion of our strategy and the reasons for the particular choice of solvent and interaction parameters. Nevertheless, we present a brief account of the main details here, which is intended to render the present publication more self-contained.

We have performed Monte Carlo simulations for two like-charged infinite planes of smeared-out surface charge density σ with counterions and solvent in between. For our choice of molecular solvent the pair potentials of the system comprise ion–ion interactions:

$$U_{\mathrm{ii}} = \frac{1}{4\,\pi\,\epsilon_0} \sum_{l=1}^{N_{\mathrm{i}}-1} \sum_{k=l+1}^{N_{\mathrm{i}}} \frac{q_l\, q_k}{r_{lk}} \tag{1}$$

ion–dipole interactions:

$$U_{\mathrm{i}\mu} = \frac{1}{4\,\pi\,\epsilon_0} \sum_{l=1}^{N_{\mathrm{i}}} \sum_{k=1}^{N_{\mathrm{d}}} q_l \frac{\boldsymbol{\mu}_k \cdot \boldsymbol{r}_{lk}}{r_{lk}^3} \tag{2}$$

and dipole–dipole interactions:

$$U_{\mu\mu} = \frac{1}{4\,\pi\,\epsilon_0} \sum_{l=1}^{N_{\mathrm{d}}-1} \sum_{k=l+1}^{N_{\mathrm{d}}} \frac{\boldsymbol{\mu}_l \cdot \boldsymbol{\mu}_k}{r_{lk}^3} - \frac{3\,(\boldsymbol{\mu}_l \cdot \boldsymbol{r}_{lk})(\boldsymbol{\mu}_k \cdot \boldsymbol{r}_{lk})}{r_{lk}^5} \tag{3}$$

where N_{i} and N_{d} are the numbers of ions and dipoles in the slit, respectively, and $r_{lk} = |\boldsymbol{r}_{lk}| = |\boldsymbol{r}_l - \boldsymbol{r}_k|$. In the PM the solvent enters the picture only through its dielectric constant ϵ_r, scaling all charge–charge interactions. All particles further interact with each other through a Lennard-Jones 12-6 potential:

$$U_{\mathrm{LJ}} = 4\,\varepsilon \left[\left(\frac{\varsigma}{r_{lk}} \right)^{12} - \left(\frac{\varsigma}{r_{lk}} \right)^{6} \right] \tag{4}$$

with $\varepsilon = 0.1\,k_{\mathrm{B}}T$ and $\varsigma = 4.0$ Å, and with the walls via a Lennard-Jones 9-3 potential:

$$U_{\mathrm{LJ\,wall}} = \frac{A}{z^9} - \frac{B}{z^3} \tag{5}$$

where z is the perpendicular distance between a particle and a wall. A and B are obtained by integration over a wall composed of the same kind of LJ particles as the ones in solution, at cubic close packing [20]. One gets $A = 2.56 \times 10^7$ J mol^{-1} Å^9 and $B = 4.69 \times 10^4$ J mol^{-1} Å^3.

The PM simulations are run in the canonical ensemble, but in the MS solvent particles are allowed to enter and leave the slit through grand canonical insertion and deletion

moves [21]. The particle translational moves are accepted or rejected according to the standard Metropolis algorithm [22]. In the case of the dipoles this translation is coupled to a rotation about one of the molecule-fixed axes. Periodic boundary conditions are applied in the x, y directions, parallel to the walls. For the truncation in the calculation of the direct particle–particle interactions we use the minimum-image convention [21]. Long range corrections are dealt with using the charged-and polarized-sheets method [13, 16, 23]. In this method the particles in the box interact with the mean charge and dipole distributions outside the simulation box.

The net osmotic pressure between the plates is given by the difference between the pressure of the confined solution and that of the bulk [24]:

$$P_{\mathrm{osm}} = P_{\mathrm{osm}}^{\mathrm{conf}} - P_{\mathrm{osm}}^{\mathrm{bulk}}. \tag{6}$$

The pressure in our slit systems was calculated both at the walls and at the midplane. In the first case one makes use of a modified version of the contact value theorem for ion–dipole mixtures [13, 25], which is

$$P_{\mathrm{osm}}^{\mathrm{conf,W}} = \mathrm{LJ_{iW}} + \mathrm{LJ}_{\mu\mathrm{W}} - \frac{\sigma^2}{2\,\epsilon_0} \tag{7}$$

where $\mathrm{LJ_{iW}}$ and $\mathrm{LJ}_{\mu\mathrm{W}}$ are the pressures corresponding to the sum of all the ion–wall and dipole–wall Lennard-Jones forces, respectively, $F_{\mathrm{LJ_{iW}},\,\mu\mathrm{W}} = -\partial\, U_{\mathrm{LJ\,wall}}/\partial\, z$ and the last term on the rhs is the electrostatic Maxwell term. This is also scaled by ϵ_r in the case of PM simulations. When evaluated at the midplane the pressure consists of a larger number of components:

$$\begin{aligned} P_{\mathrm{osm}}^{\mathrm{conf,MP}} &= \mathrm{IDEAL_i} + \mathrm{IDEAL}_\mu + \mathrm{LJ_{ii}} + \mathrm{LJ_{i\mu}} \\ &\quad + \mathrm{LJ}_{\mu\mu} + \mathrm{EL_{ii}} + \mathrm{EL_{i\mu}} + \mathrm{EL}_{\mu\mu} + \mathrm{EL_{iiout+W}} \\ &\quad + \mathrm{EL_{i\mu out}} + \mathrm{EL}_{\mu\mathrm{iout}} + \mathrm{EL}_{\mu\mu\mathrm{out}} + \mathrm{LJ_{iW}} + \mathrm{LJ}_{\mu\mathrm{W}}. \end{aligned} \tag{8}$$

The first two terms are the ideal entropic pressures of the corresponding species, i.e. $\mathrm{IDEAL_i} = k_{\mathrm{B}}T[\mathrm{i}]_{\mathrm{mid}}$, with $[\mathrm{i}]_{\mathrm{mid}}$ representing the concentration of ions at the midplane, and similarly for the dipoles. $\mathrm{LJ_{ii}}$ is the sum of the direct Lennard-Jones forces (divided by the area) between ions in opposite half-spaces, and similarly for the $\mathrm{LJ_{i\mu}}$ and $\mathrm{LJ}_{\mu\mu}$ terms. The $\mathrm{EL_{ii}}$, $\mathrm{EL_{i\mu}}$ and $\mathrm{EL}_{\mu\mu}$ correspond to the direct electrostatic forces for the same pairs of particles. $\mathrm{EL_{iiout+W}}$ is the sum of the forces (divided by the area) of ions in each half-space with the wall and external ion distribution in the other half-space. The reason for lumping these two terms together is connected to the details of the charged-sheets method and will not be elaborated on here (for details see [13, 16]). $\mathrm{EL_{i\mu out}}$ is the force between the ions in each half of the box and the external dipole distribution in the other half, and a similar notation is used for dipoles inside and ions outside and dipoles inside and dipoles outside. The $\mathrm{LJ_{iW}}$ and $\mathrm{LJ}_{\mu\mathrm{W}}$ are similar in nature to the ones in equation (7), except that here one considers only the forces between particles in each half-space and the wall in the opposite half-space. The explicit formulae for all pressure terms are given in [13].

In order to analyse the pressure at the midplane, it is convenient to group contributions into different terms. This can, of course, be accomplished in many ways. Here we have chosen to analyse the following combinations:

$$P^{\mathrm{ID}} = \mathrm{IDEAL_i} + \mathrm{IDEAL}_\mu \tag{9}$$

$$P_{\mathrm{pp}}^{\mathrm{LJ}} = \mathrm{LJ_{ii}} + \mathrm{LJ_{i\mu}} + L\,J_{\mu\mu} \tag{10}$$

$$\begin{aligned} P^{\mathrm{EL}} &= \mathrm{EL_{ii}} + \mathrm{EL_{i\mu}} + \mathrm{EL}_{\mu\mu} + \mathrm{EL_{iiout+W}} + \mathrm{EL_{i\mu out}} \\ &\quad + \mathrm{EL}_{\mu\mathrm{iout}} + \mathrm{EL}_{\mu\mu\mathrm{out}}. \end{aligned} \tag{11}$$

The $\mathrm{LJ_{iW}}$ and $\mathrm{LJ}_{\mu\mathrm{W}}$ in the case of the pressure evaluated at the midplane do not contribute significantly to the analysis, as will be exemplified below, and have therefore been left out.

An important aspect in the interpretation of the results is to consider not only the absolute value of a certain pressure term at a given separation, but especially its net value. This is defined as the difference between the absolute value at that separation and the corresponding bulk value. In the case of terms for which it does not make sense to talk in terms of bulk values we use the infinite separation value. Examples are the Maxwell and $\mathrm{LJ_{iW}}$ terms, in the case of the pressure at the walls. At infinite separation, in the PM, these will have exactly the same absolute value, but opposite sign. The values have to cancel, since at infinite separation one should attain bulk pressure, but strictly speaking they have a non-zero absolute value for a simulation of ions between charged plates. In the MS, $\mathrm{LJ}_{\mu\mathrm{W}}$ does not converge to a bulk value (i.e. the value for a simulation of dipoles only between two uncharged plates), but to a specific value for a simulation of ions and dipoles between charged surfaces. The sum of the three relevant pressure terms will, of course, go towards the bulk pressure, but this is not valid for the separate parts. In this case we will also define the net value of $\mathrm{LJ}_{\mu\mathrm{W}}$ with respect to infinite separation, not with respect to the bulk value for a dipole-only simulation.

All simulation results presented are for a box size of 44.721 Å at 298 K. We report data for two counterion valencies ($q = 0.1\,e$ and $q = 0.2\,e$, referred to as monovalent and divalent) and two surface charge densities ($\sigma = -0.001\,e$ Å^{-2} and $\sigma = -0.002\,e$ Å^{-2}, low and high surface charge density, respectively). For the primitive model results we take $\epsilon_r = 1.1$ as our low screening and $\epsilon_r = 7.0$ as the high one. We want all our simulations to share a similar primitive model description, which means that we have to be able to calculate the ϵ_r corresponding to a certain μ and dipolar number density n. We have used the Debye equation [26], which is sufficiently accurate for the chosen parameter regime. For a given μ, n is tuned to give the desired ϵ_r, via adjusting the external chemical potential, for a simulation of solvent only between uncharged walls, at large wall–wall separation. In our low density simulations we use $n = 0.006/0.008$ particles Å^{-3} at low (0.4 D) and high (1.6 D) μ, respectively. The Debye equation gives $\epsilon_r = 1.1$ for low μ and $\epsilon_r = 7.7$ for high μ. In the high density cases $n = 0.011$ particles Å^{-3} and $\mu = 0.4$ D or $\mu = 1.3$ D, corresponding to $\epsilon_r = 1.2$ or $\epsilon_r = 6.6$, respectively. The interaction parameters chosen are such that the maximum charge–charge interaction is of the same order of magnitude as for $q = 1\,e$ and $q = 2\,e$ in $\epsilon_r \sim 78$ 'water'. The maximum ion–dipole interaction energy is of the order of $k_{\mathrm{B}}T$. These represent, of course, a big technical simplification in the simulations. Furthermore, our main interest at this stage is to

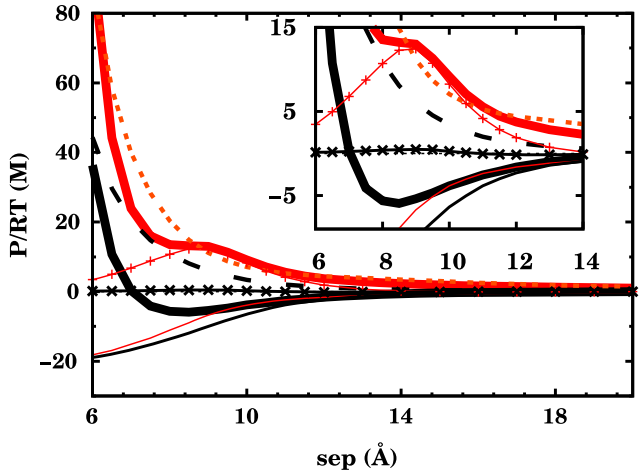

Figure 1. Net osmotic pressure and different pressure components as a function of plate–plate separation as calculated at the midplane. All curves in red (grey in the printed version) correspond to $q = 0.1\,e$, $\sigma = -0.002\,e$ Å^{-2} and $\epsilon_r = 1.1$. In black one has the results for $q = 0.2\,e$, all other parameters being equal. Thick solid lines are the net osmotic pressure, thin solid lines the P^{EL} terms. For P^{ID} one uses dashed lines and for $P^{\mathrm{LJ}}_{\mathrm{pp}}$ the lines with symbols. The inset corresponds to an upscaled plotting of one particular section of the original graph. Primitive model results.

keep the description as simple as possible, so as to facilitate the interpretation of similarities and differences resulting from the change in the level of description when going from PM to MS. The bulk pressures in the MS were calculated in simulations for solvent only between uncharged plates at 45 Å separation.

3. Results

3.1. Counterion valency effects

Figure 1 shows the net osmotic pressure between the two charged plates and the pressure components as defined in equations (9)–(11) for two different counterion valencies, in the primitive model. The first observation is that one reproduces the known ion–ion correlation attraction, namely at sufficiently high surface charge density and low enough dielectric screening, the net pressure curve has a minimum at short range, for divalent counterions, which is lost when halving the counterion valency. From the different pressure components, one realizes that the difference between monovalent and divalent curves, at the position of the correlation minimum, is not an electrostatic effect, but rather the result of the P^{ID} and $P^{\mathrm{LJ}}_{\mathrm{pp}}$ terms. If one looks at the values at 8 Å separation, the red P^{EL} curve has been slightly shifted up as a result of an increased $\mathrm{EL_{ii}}$ term (6.4 M versus 8.9 M for $q = 0.2\,e$ versus $q = 0.1\,e$, respectively). At the same separation, the two remaining components differ by about 10 M each (10.8 M for $q = 0.2\,e$ versus 20.3 M for $q = 0.1\,e$ for P^{ID} and 0.4 M versus 10.7 M for divalent and monovalent, respectively, in the case of $P^{\mathrm{LJ}}_{\mathrm{pp}}$). The divalent curve would not be net attractive without the negative electrostatic component. However, here we are focusing on the differences between pairs of curves, and in this respect the electrostatic attraction is nearly unchanged and an extra repulsion comes about in shifting the $q = 0.1\,e$ curve up. The behaviour is mainly connected to the difference in the number of counterions in the system.

It is also interesting to elaborate on the different sub-contributions to the P^{EL} term. At large separations this will tend to zero. The $\mathrm{EL_{ii}}$ term will become smaller and smaller, since the counterions will have a tendency to be 'condensed' on both walls as the distance to the opposite half-space is growing. On the other hand, the $\mathrm{EL_{iiout+W}}$ will also tend to zero. At large distances an ion on one side of the midplane will just see a smeared-out charge distribution with total charge equal to that on the wall, but of opposite sign. Since the field outside an infinite plane of smeared-out σ is independent of distance, these two forces cancel. The $\mathrm{EL_{iW}}$ term is, in fact, a constant throughout the whole separation, equal to the Maxwell term. Let us now focus on the net pressure components. From this point of view, the $\mathrm{EL_{iW}}$ term has no contribution to the pressure. As one shortens the separation between the plates, the net attractive character of the P^{EL} term can be interpreted as follows. In the mean field the ions in one half-space see a smeared-out ion distribution in the other half. In the primitive model, in the particular case of the charged-sheets method, one has the sum of an external smeared-out charge distribution and the direct charge–charge interactions in the simulation box. Due to ion correlations, the repulsion between charges on opposite half-spaces is reduced as compared to the mean-field (valid at infinite separation) behaviour. This then gives rise to a net electrostatic attraction. Similar statements have been made by Valleau *et al* [16]. The take-home message is that the net behaviour should not be interpreted in terms of an ion–wall attraction, but rather as a result of the deviations of the ion distribution in the PM (explicit, mobile counterions) when compared to the mean field. Obviously, the ion–wall term is the only attractive charge–charge interaction, but it is the deviation of the ion–ion repulsions from the mean-field/infinite separation value that allow this constant attraction to dominate over the repulsion between the mobile charges. At short separations, the P^{EL} term converges to the Maxwell term (−21.3 M), as it should. If there would be only space for a monolayer of ions between the two charged walls, all with the same z coordinate, then the z component of the direct electrostatic ion–ion interaction in the box and of the interaction of ions inside the box with ions outside would be zero. The $\mathrm{EL_{ii}}$ term is then zero both at very large and very small separations, having non-zero (positive) values in intermediate regimes. $\mathrm{EL_{iiout}} = \sigma^2/2\epsilon_0$ at infinite separation and 0 at zero separation. In the two cases being analysed here, at 20 Å, $\mathrm{EL_{ii}} \sim 12.5$ M for divalent and $\mathrm{EL_{ii}} \sim 13.5$ M for monovalent, $\mathrm{EL_{iiout+W}}$ being of similar magnitude, but with opposite sign. In other words, even if the terms just go to zero at infinity, at relatively short separations one is already in a regime where their effects nearly cancel.

We now move to the analysis of the corresponding molecular solvent curves, displayed in figure 2. Panels (a) and (b) compare the midplane situation for two different solvent densities. The pressure curves are oscillatory, as a result of packing effects. We have reported before [13], however, that the oscillations are more pronounced than for

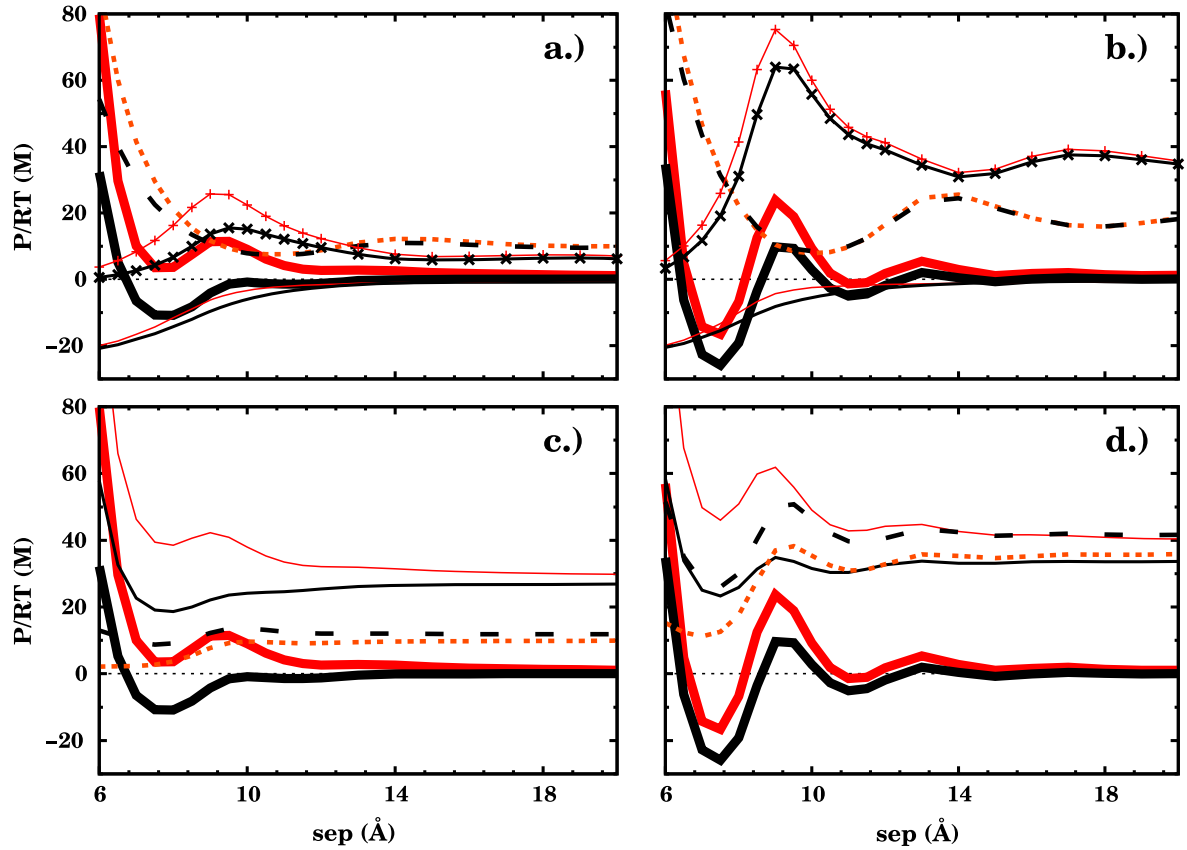

Figure 2. Net osmotic pressure and pressure components at the midplane (upper panels) and at the walls (lower panels) for low (left panels) and high (right panels) solvent density. As in figure 1, red (grey in the printed version) is used for monovalent and black for divalent counterions, and σ is also $-0.002e$ Å^{-2}. At low density $\epsilon_r = 1.1$ and at high density $\epsilon_r = 1.2$, as calculated through the Debye equation. For the upper panels the same line styles as in figure 1 are used, i.e. thick solid lines are the net osmotic pressure, thin solid lines the $P^{\rm EL}$ terms, for $P^{\rm ID}$ one uses dashed lines and for $P^{\rm LJ}_{\rm pp}$ the lines with symbols. For the lower panels the thin solid lines correspond to the $\rm LJ_{iW}$ terms and the dashed ones to the $\rm LJ_{\mu W}$ terms. The bulk pressure subtracted to obtain the net osmotic pressure was 15.2 M for low density and 51.8 M for high density.

a solvent-only system, i.e. they result from the interplay between ion and solvent packing. In any case, the qualitative ion–ion correlation attraction picture is clearly discernible. At both densities, the net pressure curves are shifted up at the position of the innermost minimum when going from divalent to monovalent counterions. Again, the electrostatic contribution to the effect is not dominant and the major difference comes from the $P^{\rm LJ}_{\rm pp}$ terms (19.1 M and 25.9 M for divalent and monovalent, respectively, in the high density molecular solvent, at 7.5 Å). This is similar to the behaviour previously observed in the PM. One should also add that, like in the PM, the difference in $P^{\rm LJ}_{\rm pp}$ is given by the $\rm LJ_{ii}$ term. At 7.5 Å one has $\rm LJ_{ii} = 13.1$ M for monovalent and 0.8 M for divalent. At 9 Å one has 18.8 M for $q = 0.1\,e$ and 1.2 M for $q = 0.2\,e$. The ion–ion term is dominant in these two extremes for different reasons, though. At 7.5 Å both the $\rm LJ_{i\mu}$ and $\rm LJ_{\mu\mu}$ differ little between monovalent and divalent. The former amounts to 12.8 M for $q = 0.2\,e$ and to 11.6 M for $q = 0.1\,e$, whereas the latter is 5.5 M for divalent and 1.1 M for monovalent. At 9 Å, however, the terms differ a lot more, but these effects act in opposite directions. $\rm LJ_{i\mu} = 34.7$ M for $q = 0.2\,e$ and 44.0 M for $q = 0.1\,e$ and $\rm LJ_{\mu\mu} = 28.1$ M for $q = 0.2\,e$ and 12.5 M for $q = 0.1\,e$. The $P^{\rm ID}$ terms, however, tend to be less and less different the more the density goes up, since the space left free by the ions on doubling the valency is being filled by dipoles.

Having analysed what is different between curves for different counterion valencies, it is now important to identify what is common, as one increases the density. In going from the primitive model to the high density molecular solvent, the $P^{\rm LJ}_{\rm pp}$ terms at 7.5 Å have gone from net repulsive to net attractive. This is connected to the increase in the bulk value (reflecting $\rm LJ_{\mu\mu}$), since the absolute value at the position of the minimum has also increased. In going from the PM to the high density MS, the depth of the $q = 0.2\,e$ minimum in the net pressure curves has increased and the $q = 0.1\,e$ curve has been shifted down and turned into net attractive, at the same separation. We can now see that this is connected to solvent depletion. In the high density molecular solvent, the pressure zero at around 10 Å corresponds roughly to the situation where two molecules can be side by side (in the z direction) in the slit, without excluded volume repulsion. Compressing them even further leads to an increase in pressure, until a maximum is reached. Between the maximum and the minimum the amount of solvent corresponding roughly to a layer of molecules abandons the slit, leaving one layer of

molecules only between the walls, which gives rise to a large reduction in their number and in P_{pp}^{LJ}. For a situation of one molecular layer only between the walls P_{pp}^{LJ} is greatly reduced, since particles are, on average, more 'under' each other than facing each other and, thereby, the z component of the LJ forces is smaller and smaller. It would be zero in the extreme, were all the particles at the same z coordinate. The appearance or increase of the large repulsive maximum at around 9 Å is in this way also connected to P_{pp}^{LJ}, namely to its increase above the bulk value as the density increases. We stress that these effects operate in roughly the same way for both ion valencies. This whole analysis is then useful in separating solvent packing or depletion effects from the coexisting ion–ion correlation attraction.

Grand canonical Monte Carlo simulations of dense Lennard-Jones fluids between neutral walls were performed long ago by Snook and van Megen [27–29]. Their studies focused on the solvation forces associated with the removal of successive layers of fluid, characterized by an oscillatory pattern, with minima and maxima. The non-specific packing and depletion effects just described are connected to this picture, albeit operating in a more complex system.

As mentioned, the LJ_{iW} and $LJ_{\mu W}$ components of the pressure at the midplane have been excluded from the analysis. Their sum constitutes an attractive term, which only becomes repulsive at the shortest separations of all (6 Å), where the behaviour is anyway dominated by the ideal entropic pressure. In the primitive model, $LJ_{iW} + LJ_{\mu W} = -3.3$ M for $q = 0.2\,e$ and -6.4 M for $q = 0.1\,e$, at 8 Å separation. As we increase the particle number density, the difference between monovalent and divalent cases is smaller and smaller, and for our high density molecular solvent $LJ_{iW} + LJ_{\mu W} = -9.0$ M for $q = 0.2\,e$ and -9.8 M for $q = 0.1\,e$, at 7.5 Å. The contribution for the difference between different valency cases is then always small and tends to disappear with density in the molecular solvent. The increase in the absolute value of the term in going from PM to MS is much smaller than other effects being analysed, namely solvent depletion. We do not believe there is that much to learn from these terms, hence their exclusion from our analysis.

Panels (c) and (d) in figure 2 present the net osmotic pressure as calculated at the walls and the corresponding pressure components. The Maxwell terms are not displayed since they are just a constant function equal to -23.4 M. The curves for the PM were not presented before since in this case the total curves correspond to the LJ_{iW} term, and can then be analysed as such. They are of course shifted down by the Maxwell term (-21.3 M), which must be equal to the infinite separation value of LJ_{iW}, in order to reach the proper bulk pressure (zero in this model). In the PM one clearly sees that at the walls the difference between monovalent and divalent is due to LJ_{iW} at the position of the minimum: it is net attractive for $q = 0.2\,e$ and net repulsive for $q = 0.1\,e$. The shape of the Lennard-Jones potential, and the fact that we are always, on average, on the repulsive branch (absolute values of the LJ_{iW} pressure always bigger than zero), necessarily means that a net attractive particle–wall term corresponds, at that position, to a closer proximity of the particles to the midplane (as compared to neighbouring positions). This is yet another clear view on the ion–ion correlation effect. For monovalent the picture conforms more to that of two double layers being squeezed more and more against the walls. For divalent, the possibility of correlations in the positions of the ions leads to a situation where the total energy of the system is actually reduced by reducing the average separation of the charges in the z direction. In the MS, despite the superimposed oscillations, the net character of the LJ_{iW} terms, at the position of the minima, is maintained. As the density increases, the $LJ_{\mu W}$ terms become more net attractive at the position of the minima, but in a similar way for both monovalent and divalent counterions. The difference between the value at 7.5 Å and that at 20.0 is -15.6 M for $q = 0.2\,e$ and -13.3 M for $q = 0.1\,e$. This is the non-specific solvent depletion effect already mentioned before. One can see that the ion–wall profiles for the monovalent cases at around 7.5 Å also develop a local minimum at high density. Again, this means a relatively closer proximity to the midplane and is connected to the ions being able to occupy the space left by the dipoles. One can also note that the infinite separation values of LJ_{iW} are increasing with increasing density. The same is valid in general throughout the whole separation regime. Again, taking into account the nature of the potentials involved, this means that the solvent spheres are effectively pushing the ions closer to the walls. We also see that the effect is felt more at higher counterion density ($q = 0.1\,e$ case).

Comparing the interpretation of the net osmotic pressure curves in terms of the components at the walls and at the midplane, it is clear that the latter analysis proves much more physically insightful. Even if the former gives a fingerprint of a correlated situation in terms of a net attractive LJ_{iW} component, as opposed to a net repulsive one for a non-correlated case, the link with the specific interactions in the system is at least diffuse. This was, of course, to be expected, taking into account the large reduction in the total number of pressure components in going from one analysis to the other. Whereas the components of the pressure at the walls just reflect the average positions of the particles, the ones at the midplane are directly derived from the different pairs of interactions in the system. In particular, the pressure at the walls interpretation is not able to discriminate whether the analysed counterion valency effects have an energetic/electrostatic origin or if they are more dependent on the different number of counterions in a monovalent as compared to a divalent system.

3.2. Screening effects

Figure 3 presents PM and high density molecular solvent results for the net osmotic pressure, at $q = 0.2\,e$, $\sigma = -0.002\,e$ Å^{-2} and two different values of ϵ_r (PM) or μ (MS). The results for low screening are the ones already given in the previous section, and are repeated here to make the comparison easier. In the PM, at the midplane, the loss of the ion–ion correlation attraction is seen to be exclusively an electrostatic effect. Neither the P^{ID} nor the P_{pp}^{LJ} terms differ significantly between $\epsilon_r = 1.1$ and 7.0. Upon reduction of the electrostatic attraction, the ideal entropic factor takes over and the net curve is shifted up. The interpretation of this reduction, in the PM, is

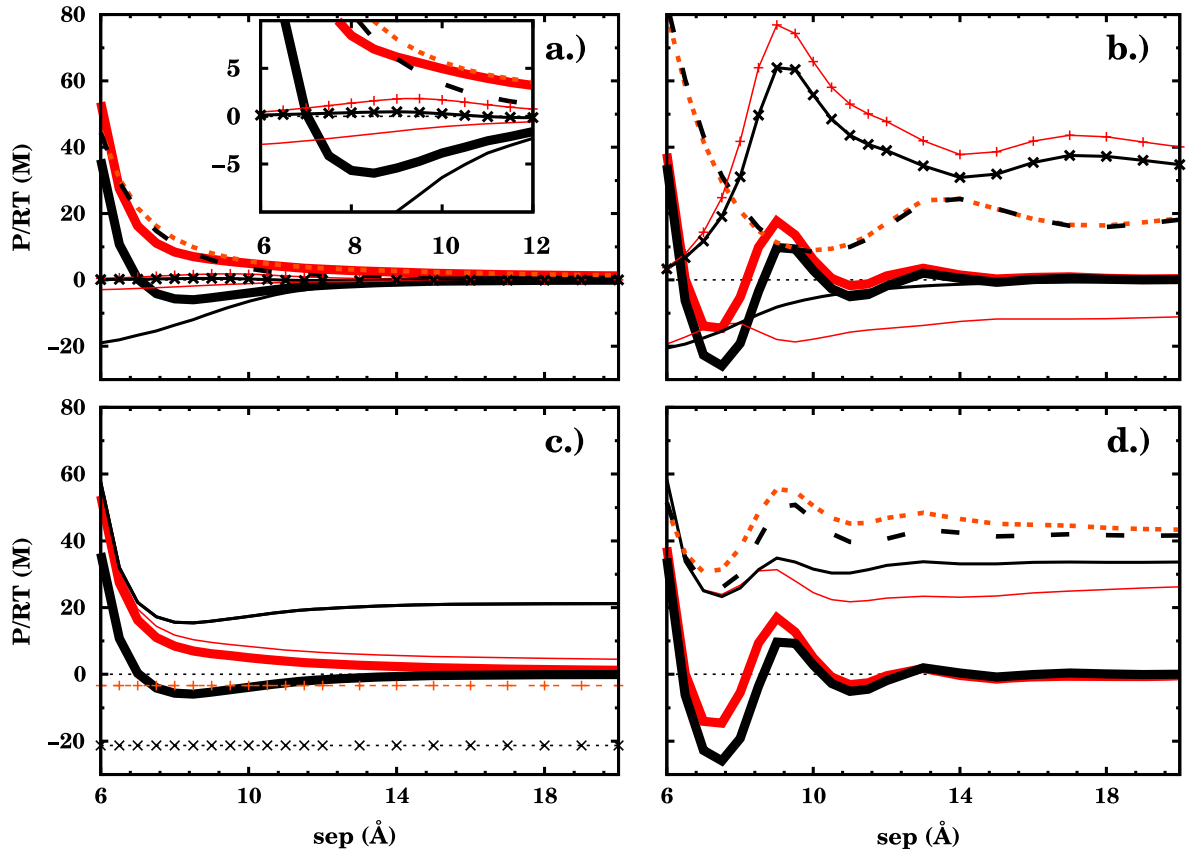

Figure 3. P^{osm} and pressure components for high surface charge density and divalent counterions, at two different values of ϵ_r. Black corresponds to low screening and red (grey in the printed version) to high screening. Left panels correspond to PM results at $\epsilon_r = 1.1$ and 7.0. In the right panels we present the results for the high density molecular solvent, for which the Debye equation gives values of the bulk ϵ_r of 1.2 and 6.6. Upper panels correspond to the pressure at the midplane. For these the thick solid lines represent the net osmotic pressure, the thin solid lines the P^{EL} terms, the dashed lines P^{ID} and the lines with symbols $P^{\mathrm{LJ}}_{\mathrm{pp}}$. For the lower panels (pressure at the walls) thin solid lines represent the $\mathrm{LJ}_{\mathrm{iW}}$ terms and the dashed ones $\mathrm{LJ}_{\mu\mathrm{W}}$. In panel (c) the dashed lines with symbols are the different Maxwell terms. The bulk pressure subtracted to obtain the net osmotic pressure was 46.6 M for the high screening case. As before, the inset in panel (a) is just an upscaled version of a particular section of the original plot.

obvious: all the electrostatics have been scaled down by ϵ_r. In the MS, the screening effect, this time related to an explicit change in the dipole moment of the solvent molecules, and not to a direct scaling of the charge–charge interactions by a constant, is still governed by the electrostatics. However, the P^{EL} curves, at 7.5 Å, are nearly coincident in absolute value. In fact, the charge–charge terms differ by less than 0.2 M. This is perfectly understandable, since the number of solvent molecules at this separation is very far away from the conditions under which the concept of a bulk dielectric constant is derived. One has, on average, not much more than 1 dipole per ion. Despite this, the bulk values of the electrostatic components are very different in the two cases, and this renders the net effect very similar to that in the PM. The bulk electrostatics stem from $\mathrm{EL}_{\mu\mu}$, which amounts to 0.1 M at 20 Å for $\mu = 0.4$ D and to -9.4 M for $\mu = 1.3$ D. The dipolar cohesivity is making all the difference. This explains the agreement between the PM and the MS picture in a situation where the amount of solvent in the slit is unable to screen charge–charge interactions in the way ϵ_r conveys. A similar net effect has a different physical origin in the two models.

The pressure decomposition at the midplane further shows the importance of ion–dipole interactions. At 7.5 Å, for example, the charge–charge terms are nearly identical. Nevertheless, the P^{EL} curve for $\mu = 1.3$ D is clearly above the one for $\mu = 0.4$ D in absolute value. The extra repulsion is mostly coming from a $\mathrm{EL}_{\mathrm{i}\mu}$ amounting to 2.8 M, and which is equal to 0.3 M for the lower dipole moment. We note that this contribution, even if not being dominant in the difference between the two P^{EL} curves in the simulations carried out in this work, is expected to be more and more important for higher charges (higher ion–dipole force). At 9 Å the relative position of the two electrostatic component curves is reversed. At this point, the dominant contribution for this is not yet the $\mathrm{EL}_{\mu\mu}$ term (-0.1 M for $\mu = 0.4$ D versus -5.4 M for $\mu = 1.3$ D), but rather $\mathrm{EL}_{\mathrm{i}\mu}$ (-0.7 M for $\mu = 0.4$ D versus -6.5 M for $\mu = 1.3$ D). The inversion in the sign of the $\mathrm{EL}_{\mathrm{i}\mu}$ term with separation is connected to the nature of the ion–dipole force, which shares a common 'magic angle' effect with the dipole–dipole interaction energy (in both cases one has the interaction with a field from a dipole). In other words, the F_z component of the ion–dipole force is attractive for $\theta < 54.4°$ and repulsive for $\theta > 54.4°$, θ being the angle between the dipole vector

and the position vector of the dipole with respect to the ion. We remind that $EL_{i\mu}$ reflects the force between ions in one half-space and dipoles in the other, and add that we have confirmed polarization profiles to ensure our 'magic angle' interpretation holds. The increase in ion–dipole interactions, and in other particle–particle interactions, can also be followed in the P_{pp}^{LJ} terms. As can be seen in figure 3, panel (b), the total Lennard-Jones curve for higher dipole moment is always above the one for the lower one. For relatively short separations, this is predominantly an effect of the $LJ_{i\mu}$ term. At 7.5 Å $LJ_{i\mu} = 12.8$ M for $\mu = 0.4$ D and 16.8 M for $\mu = 1.3$ D, while $LJ_{\mu\mu} = 5.5$ M and 7.0 M for low and high dipole moment, respectively. At 9 Å $LJ_{i\mu} = 34.7$ M for $\mu = 0.4$ D and 44.8 M for $\mu = 1.3$ D; $LJ_{\mu\mu} = 28.1$ M for low μ and 30.6 M for high μ. The ion–ion Lennard-Jones terms differ by around 0.2 M. This can be interpreted as the result of a slightly increased number of dipoles at higher interaction strength. More particles will enter the slit for stronger interactions. Another interpretation is that ions and dipoles will be closer to each other, thereby increasing the Lennard-Jones repulsion. A combination of both factors is, of course, possible and likely. We note that, for example, at 9 Å the increase in μ brought about an increase in the $LJ_{\mu\mu}$ term of around 2.5 M, while for $LJ_{i\mu}$ the difference is slightly higher than 10 M. This can be taken as an indication of the importance of the last mechanism for the increase in the ion–dipole Lennard-Jones term, based on the bigger proximity of the particles, due to the stronger electrostatic interaction. One could argue that $LJ_{\mu\mu}$ would give an upper bound to the increased density effect, $LJ_{i\mu}$ probing both mechanisms (the proximity one then being more important). At larger separations the difference in the P_{pp}^{LJ} comes from the difference in $LJ_{\mu\mu}$, which can of course also be traced to stronger interactions. One should anyway add that, throughout the whole separation regime presented, the average number of dipoles in the slit, between the two dipole moment magnitudes, does not vary more than four units. The mean value of the difference in number of dipoles, for the different simulation points, is close to 2.

The $LJ_{i\mu out}$, $LJ_{\mu iout}$ and $LJ_{\mu\mu out}$ components of the pressure have not been mentioned so far. Of the systems under analysis, they are the largest for the $q = 0.2\,e$, high σ and high ϵ_r case for a high density molecular solvent. The dipole–dipole term is even here completely negligible, being smaller than 0.1 M at all separations. At 7.5 Å, both $LJ_{i\mu out}$ and $LJ_{\mu iout}$ amount to 0.4 M, their value being 0.9 M at 9 Å. These values are $\sim 10\times$ those for the same system, at low screening. In any case, they only represent a small repulsion which is insignificant in the global behaviour, and therefore their analysis has been skipped.

We now turn to an interpretation in terms of the pressure at the walls. In the PM (figure 3(c)), the loss of the correlation attraction is again connected with going from a net attractive ion–wall term to a net repulsive one. The reduction of the charge–charge interactions through ϵ_r makes it not advantageous anymore for the counterions to slightly migrate away from the walls in order to reduce the (electrostatic) potential energy of the system. Even though the Maxwell terms are displayed, they have no net contribution to the pressure. The difference in the 'bulk' (infinite separation) values of LJ_{iW} is also a measure of the charge–charge repulsion: ions which repel each other more strongly are, on average, closer to the walls (higher LJ_{iW}). In the molecular solvent at high density, the major contribution to the difference between low and high μ curves is also coming from the ion–wall component. In this case both curves are net attractive at the position of the innermost minimum. However, the difference between the value at 7.5 Å and that at 20 amounts to -10.4 M for $\mu = 0.4$ D and -2.3 M for $\mu = 1.3$ D. The fact that LJ_{iW} went from net repulsive to attractive, at high screening, when going from the PM to the MS, is justified as follows. Before, we saw how solvent depletion leaves empty space for the ions and allows them to move slightly more towards the midplane. This justified the appearance of the local minimum in the LJ_{iW} profile in figure 2 (d), in the case of $q = 0.1\,e$. This effect also operates for divalent. In the PM, the difference between the value at 8 Å and that at 20 Å, for the $q = 0.2\,e$, high σ and low ϵ_r case, is -5.2 M, to be compared to the above-mentioned -10.4 M for the corresponding case in the high density MS. However, if anything, solvent depletion is smaller for higher μ than for the lower one. The difference between the values at 7.5 Å and those at 20 Å for the $LJ_{\mu W}$ components is -15.6 M for low μ and -11.9 M for high μ. This conforms to the intuitive picture that stronger dipoles are better kept in the slit than weaker ones (stronger ion–dipole interactions). Despite this fact, one also has to take into consideration that, in going from the PM to the MS, the difference in the infinite separation values of LJ_{iW} components, between the two screenings, has been greatly reduced or, in other words, the value for high screening has increased much more than the one for low screening. In the low screening case, one has gone from $\epsilon_r = 1.1$ in the PM to $\epsilon_r = 1.0$, whereas in the higher screening case the change has been between 7.0 and 1.0. For the MS cases the ϵ_rs mentioned are the ones which go into Coulomb's law for charge–charge interactions, and not the ones calculated through the Debye equation. The point is to make clear the difference in the effect on the Maxwell terms. This explains why the curve for $\mu = 1.3$ D is more down-shifted, at the position of the minimum, when compared to the PM. However, the source of the difference between low and high screening cases is still the same in PM and MS. One should also mention that, in the low density molecular solvent (results not shown), the net value of the LJ_{iW} term at the position of the minimum, for $q = 0.2\,e$, $\sigma = -0.002\,e\,\text{Å}^{-2}$ and high screening ($\mu = 1.6$ D) is still net repulsive, the solvent depletion effect not being so strong as at higher density. The difference in the large separation values of LJ_{iW} seen in panel (d) in figure 3 is now due to ion–dipole interactions (and thereby not so strong as the ϵ_r effect in the PM). In other words, the stronger dipoles pull the ions slightly more away from the walls into the solvating solution.

As in the previous section, one easily concludes that the pressure at the walls interpretation has quite some limitations when compared to the pressure decomposition analysis at the midplane. Even if at the walls one has a clear insight into the solvent depletion phenomenon, mostly through its direct effect on the $LJ_{\mu W}$ component, but also through its indirect

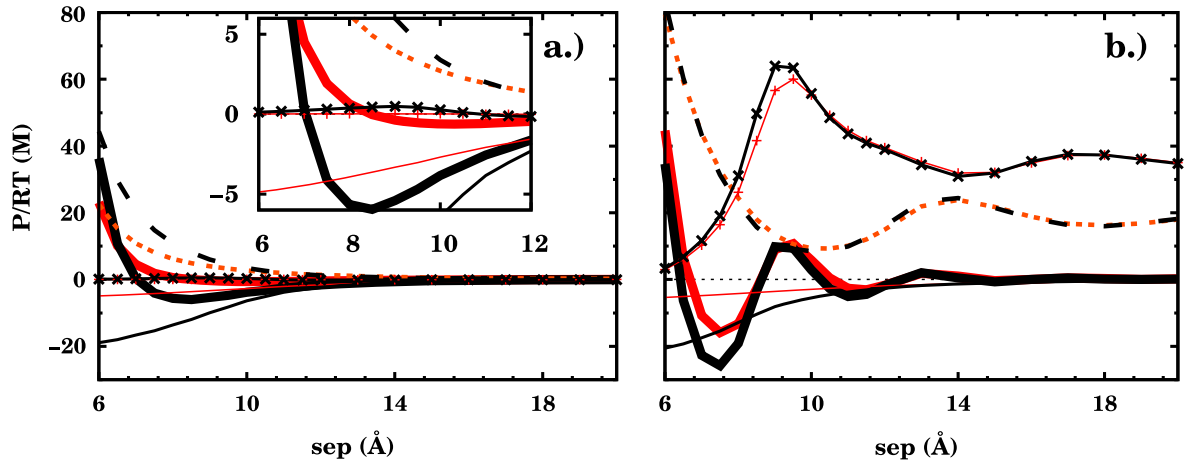

Figure 4. Pressure at the midplane and components for $q = 0.2\,e$, low screening at $\sigma = -0.002\,e$ Å^{-2} (black) and $\sigma = -0.001\,e$ Å^{-2} (red, grey in the printed version). (a) Primitive model; (b) high density molecular solvent. Following the previous notation, thick solid lines stand for the net osmotic pressure, thin solid lines for the P^{EL} terms, the dashed lines correspond to P^{ID} and the lines with symbols to $P^{\mathrm{LJ}}_{\mathrm{pp}}$. The inset in panel (a) is an upscaling of a section of the plot.

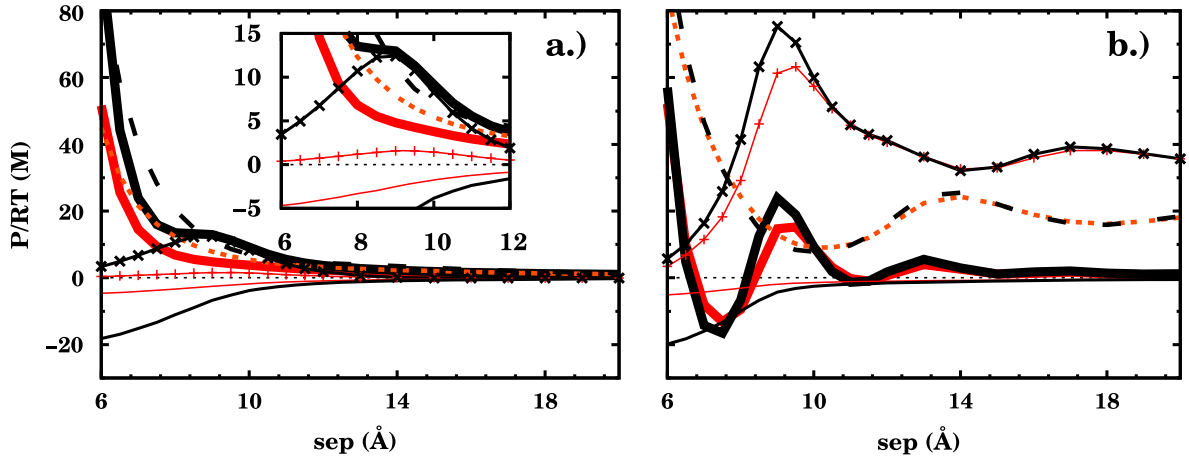

Figure 5. Pressure at the midplane and components for $q = 0.1\,e$, low screening at $\sigma = -0.002\,e$ Å^{-2} (black) and $\sigma = -0.001\,e$ Å^{-2} (red, grey in the printed version). (a) Primitive model; (b) high density molecular solvent. Thick solid lines represent the net osmotic pressure, thin solid lines the P^{EL} terms, the dashed lines are for P^{ID} and the lines with symbols for $P^{\mathrm{LJ}}_{\mathrm{pp}}$. The inset in panel (a) is an upscaling of a section of the plot.

one on $\mathrm{LJ_{iW}}$, the interpretation of the correlation attraction does not go beyond the already mentioned fingerprint kind of identification. In the MS, for high screening the ion–wall component is only weakly net attractive, while for low screening the net minimum is of the order of five times deeper. It is not at all straightforward to make the link with the already mentioned electrostatic mechanism, where the loss of the correlation effect relies on a lowering of the bulk value of the electrostatic component at high μ. The lowering of the infinite separation value of the $\mathrm{LJ_{iW}}$ component upon increased screening is, of course, connected to this, but it has more the flavour of a complement to the whole analysis, rather than of a clear identification of the underlying mechanism for the correlation attraction in this system. One also completely misses some subtleties in the behaviour of the system, like the different sign of the ion–dipole electrostatic forces, as a function of plate to plate separation, or the influence of the ion–dipole interactions on the Lennard-Jones interactions. Furthermore, in the pressure at the walls one loses the clear distinction between the two mechanisms for the correlation attraction in the PM as compared to the MS: in the first the electrostatics at large separation are very similar, and differ widely at short range. In the latter it is the bulk value which is majorly changed, the situation at short range being largely unchanged. At the walls, the big change always happens in the infinite separation value of $\mathrm{LJ_{iW}}$. Even if one knows that there is a wide difference in the electrostatic Maxwell terms in the PM, which have to cancel the infinite separation value of $\mathrm{LJ_{iW}}$, and that this difference has disappeared in the MS, this is, of course, far away from the clear mechanistic interpretation as afforded by the direct electrostatic midplane curves.

3.3. Surface charge density effects

In the primitive model, for $q = 0.2\,e$ and $\epsilon_r = 1.1$, the loss of the correlation attraction in going from $\sigma = -0.002\,e$ Å^{-2}

to $\sigma = -0.001\,e$ Å^{-2} is exclusively due to electrostatics. This is displayed in figure 4, panel (a). In fact, one even sees that there is an ideal entropic component which partly counteracts the electrostatic effect, since there is double the number of counterions per volume at higher surface charge density. The interpretation of the difference in electrostatic components is connected to the discussion of the different contributions to the P^{EL} term in the beginning of the section on counterion valency effects. The electrostatic attraction is seen as a deviation of the ion–ion repulsion from the mean-field result. The fact that the mobile ions can correlate leads to configurations of lower energies than those allowed for two opposing smeared-out double layers. In any case, however, the maximum ion–ion repulsion (mean-field result) is equal in absolute value to the attraction between ions in one half-space and the wall in the other, i.e. $\sigma^2/2\epsilon_0$. In other words, the maximum deviation cannot be bigger than the Maxwell term, which in the low surface charge density case is −5.3 M. Changing σ has therefore changed the upper bound for the correlation attraction. One again sees that the electrostatic component curves converge to these upper bounds at the shortest separations. In the MS, the difference in the two net curves at the position of the correlation minimum is again given by the electrostatic component. At this low dipole moment the electrostatics are still largely dominated by the charge–charge interactions: thus the interpretation of the difference in the two P^{EL} is as in the PM. The difference in the ideal entropic components has been erased, as usual when the space the ions leave empty when halving their number is being filled by dipoles. Until around 9 Å the small difference in the $P^{\mathrm{LJ}}_{\mathrm{pp}}$ terms is a result of the $\mathrm{LJ}_{\mathrm{i}\mu}$ component, an effect which is partly cancelled by the $\mathrm{LJ}_{\mu\mu}$ term. At 7.5 Å, $\mathrm{LJ}_{\mathrm{i}\mu} = 12.8$ M for $\sigma = -0.002\,e$ Å^{-2} and 6.8 M for $\sigma = -0.001\,e$ Å^{-2}, while $\mathrm{LJ}_{\mu\mu} = 5.5$ M and 9.6 M for high and low surface charge density, respectively. At 9 Å $\mathrm{LJ}_{\mathrm{i}\mu}$ went from 34.7 M to 18.0 M and $\mathrm{LJ}_{\mu\mu}$ from 25.1 to 38.5 M when going from high to low σ, respectively. The pressure at the walls' results are not shown but once more the difference in behaviour can be linked in both models to the $\mathrm{LJ}_{\mathrm{iW}}$ term. This is clearly net attractive for $\sigma = -0.002\,e$ Å^{-2} at the position of the correlation minimum, and has close to zero net effect for low σ, at the same separation.

Figure 5 illustrates how the loss of a certain feature in going from PM to MS can also be understood in terms of pressure components. Panel (a) shows that, in the primitive model with monovalent counterions, increasing the surface charge density leads to an increased repulsion between the charged plates. In a non-correlated regime, the situation agrees with the intuitive picture of two like-charge objects repelling each other more the bigger their charge is. This results from both the P^{ID} and $P^{\mathrm{LJ}}_{\mathrm{pp}}$ counteracting the increased electrostatic attraction at higher σ. The ideal entropic and 'collisional' effects then dominate over electrostatics. For the low density molecular solvent (results not shown) the PM behaviour is still discernible, but at higher density the relative position of the two net curves, at around 7.5 Å, has been inverted (panel (b) in figure 5). The difference between the two $P^{\mathrm{LJ}}_{\mathrm{pp}}$ components being similar to that in the PM, we immediately conclude that this is an exclusively entropic effect, connected to the fact that now there is no difference in P^{ID} between both surface charge densities, as is common at high density. The difference in the Lennard-Jones terms is still dominated by the $\mathrm{LJ}_{\mathrm{ii}}$ component, either because the other two do not differ much (like at 7.5 Å) or because their differences (nearly) cancel (like at 9 Å).

4. Conclusions

We have performed a thorough and systematic comparative analysis of the different components of the pressure between two infinite like-charged plates with only counterions and solvent in between, both at the walls and at the midplane between them. This shows that the ion–ion correlation attraction operating in the primitive model for sufficiently high electrostatic coupling (high q, σ and/or low ϵ_r) is also taking place in a dipolar solvent. In fact, the same pressure components are responsible for the same effects in these two models, namely:

- counterion valency effects are not predominantly a direct electrostatic phenomenon, but are rather related to the difference in the number of counterions in the system, either through both their ideal entropy and direct excluded-volume interactions (PM) or just the latter (MS);
- screening effects are clearly of electrostatic origin, even if with a different physical mechanism in both models: in the PM changes happen in the short separation electrostatics through a direct screening of all charge–charge interactions by ϵ_r; in the MS the electrostatic interactions at short range are largely unchanged when increasing μ, and the reduction of the innermost minimum in the net pressure curves comes about through a lowering of the bulk value of the electrostatic component, due to dipolar cohesivity. This renders its net attractive effect at short separations smaller than the one at lower μ. We note that this provides an explanation as to why the PM works at short ranges, when there is almost no solvent in the slit, through a difference in bulk pressure at different values of the solvent dipole moment;
- surface charge density effects are also exclusively electrostatic, but share the same physical origin in both models. When correlation attraction is seen as a deviation from the mean-field ion–ion repulsion, changing σ has the effect of changing the upper bound for the maximum deviation (the Maxwell term, equal to the attraction between ions in one half-space and the wall in the other).

The above conclusions emerge mainly from the analysis of the pressure components at the midplane. In the pressure at the walls one basically has two components only to look at, which inevitably limits their usefulness. The Lennard-Jones interaction between ions and walls gives an interesting perspective over the correlation phenomenon. In a non-correlated situation the picture conforms to that of two double layers being pushed against each other, the counterions going more towards the walls as the distance between them is decreased, whereas in a correlated situation the ions at short range go slightly away from walls to minimize the energy of

the system. However, the differentiation between these two extremes cannot go beyond the fingerprint of having a net attractive versus a net repulsive (or weakly attractive) LJ_{iW} component, and establishing links between the interactions in the system and the resulting pressure components is not straightforward.

Pressure decomposition is also instrumental in distinguishing between solvent packing/depletion and the coexisting correlation attraction. Compared to the PM, all net pressure curves for the MS are shifted down at the position of the innermost minimum. This is a fairly non-specific effect which operates roughly in the same way for different counterion valencies, dipole moment magnitudes and surface charge densities. It is not connected to changes in electrostatic coupling but merely in density in going from PM to MS: in particular, to the difference between the bulk pressure values and those at short ranges, when one removes the second-last layer of solvent in the slit. Solvent depletion is then mainly seen in the difference between the infinite separation value of the pressure term corresponding to the total excluded-volume repulsions (P_{pp}^{LJ}) and the one at the position of the correlation minimum, in the case of the pressure at the midplane. In the case of the pressure at the walls solvent depletion manifest itself also very clearly through a net attractive dipole–wall Lennard-Jones term. Immediately before the minimum where solvent depletion and correlation attraction coexist, the curves in the MS have a net repulsive maximum. This is connected to the packing of two layers of spheres in the slit, and is obvious, for example, in the P_{pp}^{LJ} term.

It emerges from the discussion above that the interpretation of pressure components is better done in terms of net effects, defined as the difference between the bulk or infinite separation value of one component and the absolute value at a certain separation. This has a clear link with the experimental definition of osmotic pressure, and has full physical meaning in the case of the pressure at the midplane. The two best examples are perhaps the just-mentioned solvent depletion effects, which rely on the difference between a relatively high positive bulk value for P_{pp}^{LJ} and a comparatively small value at short range, rendering the net effect attractive, and the loss in the correlation attraction upon increased μ, at constant q and σ, as explained above.

The components of the pressure at the midplane also provide insight into more subtle effects directly derived from the different interactions in the system. Examples are the change in the sign of the ion–dipole electrostatic forces, at short separations and sufficiently high μ, going from repulsive to attractive, and the increase in the P_{pp}^{LJ} term due to stronger ion–dipole interactions. This last effect is, of course, connected to the bigger average proximity between the different species. Moreover, the pressure at the midplane makes it obvious that the effects of ideal entropy will disappear at high solvent density, where space left empty by ions is filled up by dipoles. A good example is the inversion of the behaviour of the systems for monovalent counterions and low screening upon changing σ, when one compares PM and MS. In the PM, the fact that two non-correlated double layers repel each other more the higher σ is depends highly on P^{ID}, hence the effect is lost at sufficiently high solvent number density.

Acknowledgment

This work was supported by the Fundação para a Ciência e a Tecnologia, Portugal (LP, SFRH/BD/21462/2005).

References

[1] Guldbrand L, Jönsson B, Wennerström H and Linse P 1984 Electrical double layer forces. A Monte Carlo study *J. Chem. Phys.* **80** 2221
[2] Kjellander R and Marčelja S 1984 Correlation and image charge effects in electric double layers *Chem. Phys. Lett.* **112** 49
[3] Verwey E J W and Overbeek J Th G 1948 *Theory of the Stability of Lyophobic Colloids* (Amsterdam: Elsevier)
[4] Jönsson B and Wennerström H 2004 Ion–ion correlations in liquid dispersions *J. Adhes.* **80** 339
[5] Hunter R J 2004 *Foundations of Colloid Science* 2nd edn (Oxford: Oxford University Press)
[6] Tang Z, Scriven L E and Davis H T 1994 Effects of solvent exclusion on the force between charged surfaces in electrolyte solution *J. Chem. Phys.* **100** 4527
[7] Otto F and Patey G N 1999 Forces between like-charged plates in electrolyte solution: ion-solvent packing versus electrostatic effects *Phys. Rev.* E **60** 4416
[8] Otto F and Patey G N 2000 Forces between like-charged walls in electrolyte solution: molecular solvent effects at the McMillan–Mayer level *J. Chem. Phys.* **112** 8939
[9] Otto F and Patey G N 2000 Forces between like-charged walls in an electrolyte solution: a comparison of Mcmillan-Mayer results for several models *J. Chem. Phys.* **113** 2851
[10] Kjellander R, Lyubartsev A P and Marčelja S 2001 McMillan–Mayer theory for solvent effects in inhomogeneous systems: calculation of interaction pressure in aqueous electrical double layers *J. Chem. Phys.* **114** 9565
[11] Kinoshita M, Iba S and Harada M 1996 Interaction between macroparticles in aqueous electrolytes *J. Chem. Phys.* **105** 2487
[12] Lee M, Chan K Y and Tang Y W 2002 Forces between charged surfaces in a solvent primitive model electrolyte *Mol. Phys.* **100** 2201
[13] Pegado L, Jönsson B and Wennerström H 2008 Ion–ion correlation attraction in a molecular solvent *J. Chem. Phys.* at press
[14] Kjellander R and Marčelja S 1986 Interaction of charged surfaces in electrolyte solutions *Chem. Phys. Lett.* **127** 402
[15] Kjellander R and Marčelja S 1986 Double-layer interaction in the primitive model and the corresponding Poisson–Boltzmann description *J. Phys. Chem.* **90** 1230
[16] Valleau J P, Ivkov R and Torrie G M 1991 Colloid stability: the forces between charged surfaces in an electrolyte *J. Chem. Phys.* **95** 520
[17] Kjellander R, Åkesson T, Jönsson B and Marčelja S 1992 Double-layer interactions in mono- and divalent electrolytes: a comparison of the anisotropic hypernetted chain theory and Monte Carlo simulations *J. Chem. Phys.* **97** 1424
[18] Pellenq R J-M, Caillol J M and Delville A 1997 Electrostatic attraction between two charged surfaces: a (N, V, T) Monte Carlo simulation *J. Phys. Chem.* B **101** 8584
[19] Delville A, Pellenq R J-M and Caillol J M 1997 A Monte Carlo (N, V, T) study of the stability of charged interfaces: a simulation on a hypersphere *J. Chem. Phys.* **106** 7275
[20] Hill T L 1986 *An Introduction to Statistical Thermodynamics* (New York: Dover)
[21] Allen M P and Tildesley D J 1987 *Computer Simulation of Liquids* (Oxford: Oxford Science Publications)

[22] Metropolis N, Rosenbluth A W, Rosenbluth M N, Teller A H and Teller E 1953 Equation of state calculations by fast computing machines *J. Chem. Phys.* **21** 1087
[23] Boda D, Chan K Y and Henderson D 1998 Monte Carlo simulation of an ion–dipole mixture as a model of an electrical double layer *J. Chem. Phys.* **109** 7362
[24] Evans D F and Wennerström H 1999 *The Colloidal Domain. Where Physics, Chemistry, Biology and Technology Meet* 2nd edn (New York: Wiley–VCH)
[25] Blum L and Henderson D 1981 Mixtures of hard ions and dipoles against a charged wall: the Ornstein–Zernike equation, some exact results, and the mean spherical approximation *J. Chem. Phys.* **74** 1902
[26] Böttcher C J F 1973 *Theory of Electric Polarization* (Amsterdam: Elsevier)
[27] Snook I K and van Megen W 1979 The solvation force between colloidal particles *Phys. Lett.* A **74** 332
[28] Snook I K and van Megen W 1980 Solvation forces in simple dense fluids. I *J. Chem. Phys.* **72** 2907
[29] van Megen W J and Snook I K 1981 Solvation forces in simple dense fluids. II. Effect of chemical potential *J. Chem. Phys.* **74** 1409